Clim Dyn (2018) 51:2113–2126
DOI 10.1007/s00382-017-4002-5

Interdecadal change on the relationship between the mid-summer temperature in South China and atmospheric circulation and sea surface temperature

Ruidan Chen[1,3,5] · **Zhiping Wen**[2,5] · **Riyu Lu**[3,4]

Received: 8 July 2017 / Accepted: 31 October 2017 / Published online: 9 November 2017

Abstract South China suffers from high temperature frequently in mid-summer and this study aims to explore the interdecadal change of interannual variation of the mid-summer temperature in South China. It is revealed that the relationship between South China temperature and atmospheric circulation and sea surface temperature anomaly (SSTA) experiences an interdecadal change around the early 1990s. Before the early 1990s, warmer summer in South China is associated with the mid-latitude teleconnection featured by higher pressure over the Ural Mountains and the Korean Peninsula and lower pressure around the Lake Baikal. South China is located at the southern flank of an anomalous high pressure. After the early 1990s, South China temperature is prominently influenced by the tropical SSTA, and meanwhile the mid-latitude teleconnection becomes much weaker. Warmer summer is associated with higher pressure centered over South China and the El Niño to La Niña transition phase. The higher pressure influencing South China is located more southwards after the early 1990s, and it is favored by the tropical SSTA. The warmer SST in summer over the western tropical Pacific enhances the local convection and triggers an anomalous local Hadley cell with stronger subsidence over South China, directly leading to higher pressure over South China. Moreover, the colder SST over the central–eastern Pacific induces an anomalous Walker circulation and further strengthens the convection over the western tropical Pacific, exerting an indirect impact on the higher pressure over South China. The relative role of the western Pacific warming and central–eastern Pacific cooling is verified by CAM4 simulations. The intimate relationship between the tropical SSTA and South China temperature occurs during the El Niño to La Niña transition phase, which is the case after the early 1990s and suggests higher predictability for South China temperature in the recent decades.

Keywords Interdecadal change · Interannual variation · Mid-summer temperature · South China

✉ Ruidan Chen
chenrd3@mail.sysu.edu.cn

[1] Center for Monsoon and Environment Research/Guangdong Province Key Laboratory for Climate Change and Natural Disaster Studies/School of Atmospheric Sciences, Sun Yat-sen University, Guangzhou 510275, China

[2] Institute of Atmospheric Sciences, Fudan University, Shanghai, China

[3] State Key Laboratory of Numerical Modeling for Atmospheric Sciences and Geophysical Fluid Dynamics, Institute of Atmospheric Physics, Chinese Academy of Sciences, Beijing 100029, China

[4] University of the Chinese Academy of Sciences, Beijing 100049, China

[5] Jiangsu Collaborative Innovation Center for Climate Change, Nanjing, China

1 Introduction

South China, located at the tropical-subtropical region influenced by East Asian monsoon, suffers from high temperature frequently in summer. The temperature in South China reaches the highest in July–August (hereafter mid-summer), with 90% of extreme heat days occurring in this period (Chen et al. 2016). The frequency of extreme heat in South China ranks high in China both in terms of the climatological frequency and increasing trend (Gao et al. 2008; Wei and Chen 2009). The high temperature in mid-summer greatly threats the human society, such as increasing human health risk, reducing crop yields and causing excessive use

of electricity resource (He et al. 2008; Zeng et al. 2011; Li et al. 2014). On the other hand, South China is characterized by highly centralized population and economics, more vulnerable to meteorological disasters. Therefore, it is important to understand the causes of mid-summer temperature variation in South China. The current study aims at the interannual variation of the mid-summer temperature in South China and investigates the interdecadal change in the influencing factors.

A preliminary analysis shows that the mid-summer temperature in South China presents large interannual variability and the interannual component contributes greatly to the original anomaly (Fig. 1). In particular, the hottest summer in 2003 is basically related to the interannual variability, with the interannual component accounting for 94% of the total warming. Moreover, the top two warmest years of the interannual component, i.e., 2003 and 1998, are also accompanied by the top two highest extreme heat (EH) frequencies (Fig. 1). Hence, it is of great significance to study the interannual variation of the mid-summer temperature in South China, which is helpful for understanding the total temperature variation and occurrence of extreme cases.

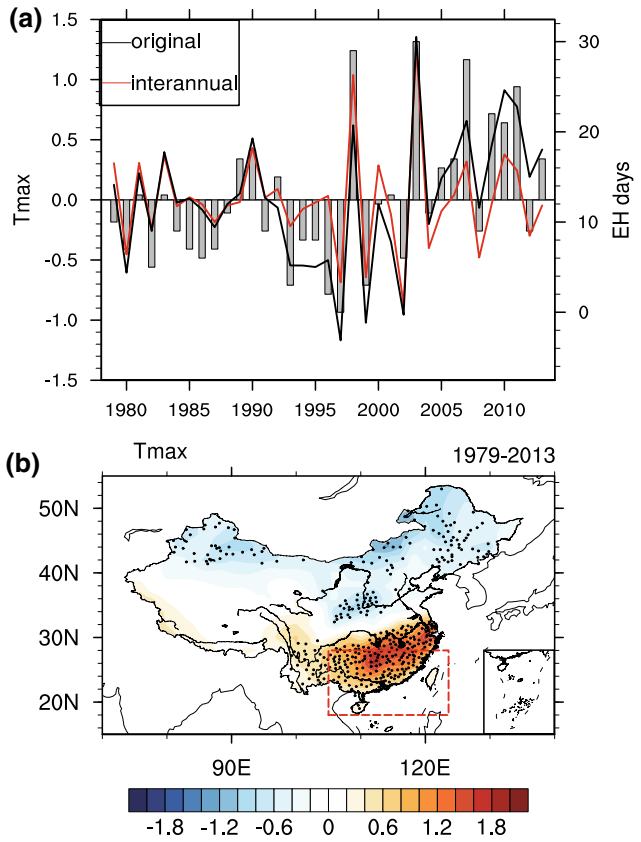

Fig. 1 **a** Mid-summer temperature anomaly averaged over the South China stations during 1979–2013 (black line) and the corresponding interannual component (red line) (units: °C), and the annual occurrence frequency of extreme heat (EH) days in South China (bars; unit: day). The counting of EH frequency is based on the definition of EH the same as Chen et al. (2016), defined as the days on which more than 1/3 of the stations in South China have T_{max} exceeding 35 °C. **b** Regressed anomaly of mid-summer temperature over the observational stations in China against the temperature anomaly in South China (units: °C). The dotted stations are significant at the 90% significant level. The red rectangle denotes the domain of South China

Some previous studies have been conducted to explore the causes of the interannual variation of mid-summer temperature in South China. On the one hand, the atmospheric circulation associated with the temperature variation presents significant geopotential height anomaly at 500 hPa over South China (Luo and Ji 2005; Yan and Huang 2005; Sun et al. 2011). Higher pressure occurs over South China in warmer years, indicating the strengthening and westward shifting of the subtropical high over the western North Pacific (Gong et al. 2004; Yang and Li 2005; Wang et al. 2016). Besides the local pressure anomaly, the variation of South China temperature is related to a wave train pattern spanning the Eurasian continent, indicating the influence from the extratropical atmospheric circulation (Luo and Ji 2005; Yan and Huang 2005; Ding and Qian 2012; Wang et al. 2013). On the other hand, the sea surface temperature (SST) over the tropical Pacific exhibits obvious anomalies corresponding to the temperature variation in South China. There is significantly warmer SST over the central–eastern tropical Pacific during the winter and spring before warmer summer in South China, appearing as an El Niño pattern (Luo and Ji 2005; Ren et al. 2011).

The influence of tropical Pacific SST anomaly (SSTA) on the East Asian monsoon circulation has been addressed extensively by previous studies. Wang et al. (2000) suggested that the warmer SST in winter over the central tropical Pacific would favor an anomalous anticyclone at the lower troposphere over the western North Pacific via a Rossby-wave response, and the anomalous anticyclone would persist until the following early summer through a positive thermodynamic air-sea feedback. But the anticyclonic anomaly only persists until early summer in presence of the mean northeasterly trades. A further study by Chen et al. (2015) suggested that the colder SST in summer over the central–eastern Pacific is important for the maintenance of the anticyclonic anomaly over the western North Pacific throughout the summer during El Niño to La Niña transition years, through a Rossby-wave response to the northwest of the colder SST. Meanwhile, the SSTA over the western tropical Pacific could directly exert an impact on the East Asian atmospheric circulation through a meridional vertical cell (Hu 1997; Sui et al. 2007). Warmer SST over the western tropical Pacific would favor stronger ascending motion over the tropics and subsequent descending motion over the western North Pacific, the latter of which implies the westward-extending of the subtropical high.

On the other hand, the summer climate in East Asia experiences a prominent interdecadal change in the early 1990s. The East Asian summer monsoon obviously weakens after the early 1990s, manifested by a significant decrease in the subtropical jet, a barotropic anticyclonic anomaly over northeastern Asia, and an anomalous meridional vertical overturning circulation over the tropical region (Kwon et al. 2007; Wang et al. 2009; Zhang et al. 2016). Meanwhile, there is a decadal modulation in the relationship between the East Asian summer monsoon, western North Pacific summer monsoon and tropical Pacific SST in the early 1990s (Kwon et al. 2005; Yim et al. 2008). Accompanying the change of summer monsoon, the precipitation over East Asia also experiences an evident interdecadal change. The dominant variability mode of summer precipitation changes from a tripolar to a dipole pattern in the early 1990s, and the precipitation over South China significantly increases since the early 1990s (Kwon et al. 2007; Ding et al. 2008; Wu et al. 2010). Moreover, the interannual variation of precipitation in South China and its influencing factors also present an obvious interdecadal change. Chen et al. (2017) revealed that the interannual variability of the summer precipitation over South China obviously increases after the early 1990s, and it is partly attributable to the increased amplitude of the eastern tropical Indian Ocean SST and the enhanced influence of the North Atlantic triple SST pattern. Yim et al. (2014) indicated that the controlling SSTA for East Asian early summer rainfall variation has also changed around the mid-1990s, characterized by a slow decay of eastern Pacific warming before mid-1990s and a rapid decay of central Pacific warming and a tripolar SST in North Atlantic after the mid-1990s.

Compared with the extensive studies on precipitation, the investigation on the interdecadal change of temperature is far not enough. Specifically, the current study aims to reveal the interdecadal change on the relationship between the mid-summer temperature in South China and the atmospheric circulation and tropical Pacific SST. The relative contribution of the SSTA over the western Pacific and central–eastern Pacific to the atmospheric circulation pattern responsible for the temperature variation in South China would also be investigated using the CAM4 model. The rest of the paper is organized as follows. Section 2 describes the data, methods and model experiments used for analysis. Section 3 reveals the interdecadal change of the relationship between South China temperature and atmospheric circulation and SSTA around the early 1990s. Section 4 presents the atmospheric circulation and SSTA responsible for the South China temperature variation during the two epochs before and after the early 1990s. Section 5 gives the conclusions.

2 Data, methods and model experiments

2.1 Data and methods

The analyzed period covers the mid-summer (July–August) from 1979 to 2013 because the temperature in South China reaches the highest in July–August (Chen et al. 2016). The data used in this study are derived from five datasets: (1) homogenized daily maximum surface air temperature (T_{max}) of 753 national standard stations in China (Li et al. 2016). South China denotes the region south of 28°N and east of 105°E including 149 stations, which is the same as Chen et al. (2016). The mid-summer temperature of South China is computed as the T_{max} averaged over the 149 stations during July–August. We have also repeated the analyses but computing the reference temperature series as the average daily mean temperature (T_{mean}) and daily minimum temperature (T_{min}), and the results turn out to be similar (not shown). (2) Monthly data of the European Center for Medium-Range Weather Forecasts Interim Reanalysis (ERA-Interim; Dee et al. 2011), with a horizontal resolution of 2.5° × 2.5°. (3) Outgoing longwave radiation (OLR) data with a horizontal resolution of 2.5° × 2.5° from the National Oceanic and Atmospheric Administration (NOAA; Liebmann and Smith 1996), which could manifest the large-scale convection. (4) HadISST monthly sea surface temperature with a horizontal resolution of 1° × 1° (Rayner et al. 2003). (5) Precipitation data with a horizontal resolution of 2.5° × 2.5° from Global Precipitation Climatology Project (GPCP).

This study focuses on the interannual variation of the mid-summer temperature in South China. Thus a 9-year high-pass filter is applied to all the variables to extract the interannual components, based on the Lanczos temporal filtering. In analysis of the patterns associated with the temperature variation, the variable anomalies are regressed onto the temperature anomaly averaged over South China. The Student's *t* test with a significant level of 90% is used for estimating the significance.

2.2 Model experiments

The Community Atmosphere Model Version 4 (CAM4) is employed in the current study, which is developed by the National Center for Atmospheric Research (NCAR) and also serves as the atmospheric component of the Community Climate System Model Version 4 (CCSM4). The CAM4 model could reasonably reproduce the mean climate, and a detailed description of the model and simulation can be found in Neale et al. (2013). The model has a horizontal resolution of approximate 1.9° latitude × 2.5° longitude and 26 vertical levels extending from the surface to near 3.5 hPa.

In order to detect the relative role of the western Pacific and central–eastern Pacific SSTA in the formation of

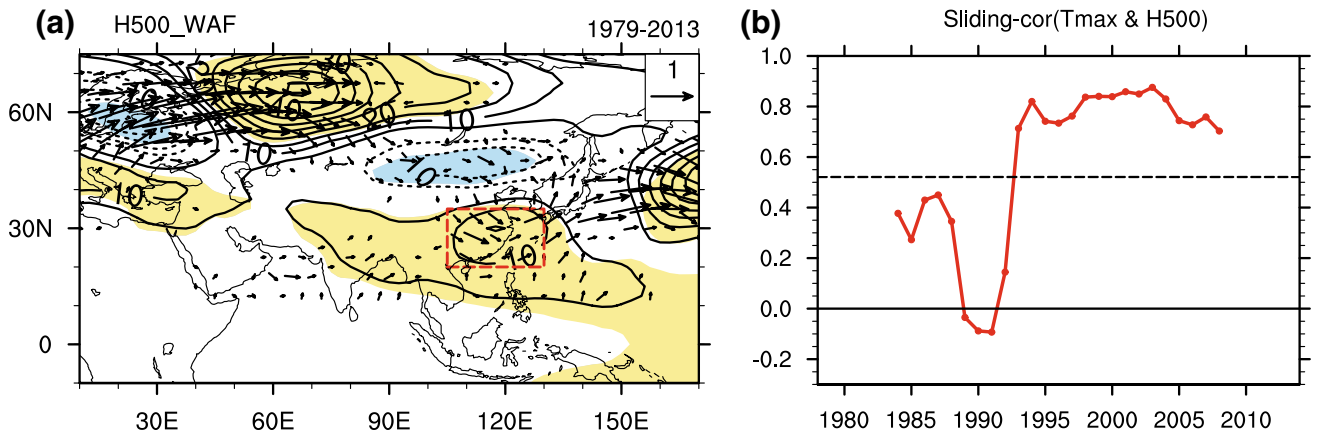

Fig. 2 **a** Regressed anomaly of 500-hPa geopotential height (contours; unit: gpm; the shading areas are significant) and the corresponding wave activity flux (vectors; unit: $m^2\ s^{-2}$; only the vectors greater than 0.1 are plotted) against the mid-summer temperature anomaly in South China for the whole period from 1979 to 2013. The yellow (blue) shading areas are statistically significant positive (negative) at the 90% significant level. The dash box is chosen as the key region of the geopotential height anomaly, covering (20°N–35°N, 105°E–130°E). **b** 11-year sliding correlation coefficient between the mid-summer temperature anomaly in South China and the geopotential height anomaly averaged over the key region. The dashed line denotes the 90% significant level

atmospheric circulation responsible for the mid-summer temperature variation in South China, four numerical simulations are performed. The first simulation is the control run (hereafter CTL run), in which the forcing SST is the observed climatological mean seasonal cycle of global SST. The other three idealized sensitivity experiments are forced by SST with anomalies during July–August added to the climatological mean upon different regions (Fig. 10a–c): (1) both an increase of 0.4 °C over the western tropical Pacific covering (10°S–10°N, 105°E–160°E) and a decrease of 0.8 °C over the central–eastern tropical Pacific covering the Niño3.4 region (5°S–5°N, 170°W–120°W) (hereafter WP_EP run); (2) only an increase of 0.4 °C over the western tropical Pacific (hereafter WP run); (3) only a decrease of 0.8 °C over the central–eastern tropical Pacific (hereafter EP run). The amplitudes and regions of SSTA are based on the simultaneous regressed SSTA pattern against the South China temperature (Figs. 3b, 7d). For western Pacific,

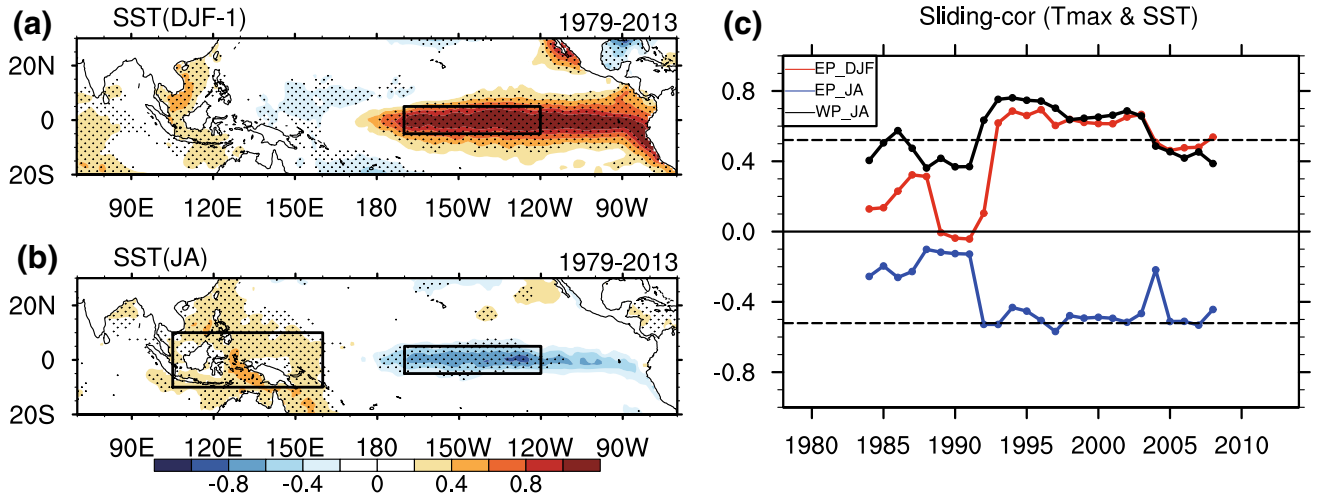

Fig. 3 Regressed SSTA in the **a** preceding winter from December to February and **b** simultaneous mid-summer from July to August against the mid-summer temperature in South China for the whole period from 1979 to 2013 (shading; units: °C). The dotted areas are statistically significant at the 90% significant level. The black boxes are chosen as the key regions of SSTA, including (10°S–10°N, 105°E–160°E) over the western tropical Pacific and Niño3.4 region (5°S–5°N, 170°W–120°W) over the central–eastern tropical Pacific. **c** 11-year sliding correlation coefficients between the mid-summer temperature anomaly in South China and the SSTA over the key regions, including the central–eastern Pacific SST during the preceding winter (red line) and July–August (blue line) and the western tropical Pacific SST during July–August (black line). The dashed lines denote the 90% significant level

only the warming between 10°S–10°N is imposed, because the SSTA within this region plays an active role to influence the atmosphere, while the SSTA beyond this latitude is a response to the atmospheric circulation, which would be deduced from Fig. 8. Each simulation is integrated for 20 years and the last 19 years are used for analysis since the first year is regarded as the spin up. The differences between the sensitivity experiments and the CTL run are calculated to manifest the forcing effect of different SSTA patterns. The Student's *t* test at 90% significant level is employed for estimating the significance.

3 Interdecadal change of the relationship between South China temperature and atmospheric circulation and SST around the early 1990s

Figure 1a exhibits the mid-summer temperature anomalies in South China spanning from 1979 to 2013 and the corresponding interannual component. It is shown that the temperature presents notable interannual variability, and the interannual component deviates from the original anomaly in many years especially since the early 1990s. Therefore, it is necessary to extract the interannual component for the current study. Hereafter, all the variables are the 9-year high-pass filtered components. The regressed anomaly of mid-summer temperature over the observational stations in China against the temperature anomaly in South China presents a dipole mode (Fig. 1b). For the warmer years in South China, there is significantly higher (lower) temperature south (north) of 30°N, manifesting a meridional connection.

Figure 2a demonstrates the regressed anomaly of 500-hPa geopotential height and the corresponding wave activity flux against the temperature anomaly in South China during 1979–2013. The geopotential height shows significantly positive anomalies over South China and around the Ural Mountains, and meanwhile negative anomalies to the south of the Lake Baikal and over Europe, forming a wave train spanning from Europe to East Asia. This mid-latitude wave train pattern is similar to the result of Luo and Ji (2005), which analyzed the composite difference between abnormally warm and cold mid-summer in South China. The wave activity flux associated with the mid-latitude wave train propagates from Europe to South China, with eastward flux from Europe to the Ural Mountains and southeastward flux from the Ural Mountains to the Lake Baikal and further to South China. Meanwhile, there is northeastward wave activity flux propagating from the low-latitude region to the higher-pressure center around South China and then further to North Pacific. It is hence implied that the higher pressure over South China results from the combined effect of the mid-latitude and tropical disturbance.

In order to detect the interdecadal change on the relationship between South China temperature and atmospheric circulation, the geopotential height anomaly averaged on the centered area (20°N–35°N, 105°E–130°E) over South China is defined as the circulation index H500, and the 11-year sliding correlation coefficient between South China temperature and H500 is calculated (Fig. 2b). It is noticeable that the correlation coefficient abruptly increases in the early 1990s: The coefficient is blow 0.45 and not significant before 1993, but above 0.7 and significant since 1993. Therefore, the relationship between South China temperature anomaly and local pressure anomaly centered over South China is only significant since the early 1990s.

Moreover, the correlation between South China mid-summer temperature and tropical Pacific SST also displays an interdecadal change around the early 1990s. Figure 3a, b demonstrates the regressed SSTA against the South China temperature anomaly for the whole period from 1979 to 2013, including the SSTA during the preceding winter and simultaneous mid-summer. The winter SSTA shows significant warming (cooling) over the central–eastern (western) Pacific, appearing as an El Niño pattern (Fig. 3a). On the contrary, the mid-summer SSTA demonstrates a La Niña pattern, with significant cooling (warming) over the central–eastern (western) Pacific (Fig. 3b). It is thus implied that the warmer summer in South China is associated with the El Niño to La Niña transition phase evolving from the preceding winter. Accordingly, we select the high correlated regions over the western tropical Pacific (10°S–10°N, 105°E–160°E) and central–eastern tropical Pacific Niño3.4 region (5°S–5°N, 170°W–120°W) as the key SST regions, and then calculate the 11-year sliding correlation coefficient between South China temperature and key-region SST. The result shows that the relationship of higher South China temperature and preceding-winter warmer SST over the central–eastern Pacific, simultaneous colder SST over the central–eastern Pacific and warmer SST over the western Pacific presents clear interdecadal changes around the early 1990s (Fig. 3c). The correlation coefficients are insignificant before 1993 or 1992, and become generally significant afterwards. Thereby, it is revealed that the relationship between South China mid-summer temperature and atmospheric circulation and tropical Pacific SST experiences an evident interdecadal change around the early 1990s. The specific characteristics associated with South China temperature anomalies in the two epochs before and after 1993 would be compared in the following.

4 Atmospheric circulation and SSTA responsible for the South China temperature variation during the two epochs before and after the early 1990s

Figure 4 exhibits the regressed anomalies of mid-summer temperature over the observational stations in China against the temperature anomaly in South China for the two epochs before and after 1993, respectively. Both epochs present a dipole mode, but differ in the meridional positions of the anomaly centers. The anomalous pattern for the second epoch is quite similar to the whole period from 1979 to 2013 (Figs. 1b, 4b), with warm center south of 30°N and cold anomaly in the north. In comparison, the anomaly centers for the first epoch obviously shift northwards (Fig. 4a). The warm center is located along the Yangtze River at 30°N, and the cold anomaly also migrates northwards to north of 38°N. It is noticed that the positive correlation along the coast of southeast China is weak during the first epoch and it is related to the interdecadal change in the main variability mode of South China temperature. An Empirical Orthogonal Function (EOF) analysis on the interannual component of the temperature anomalies over South China is performed for both epochs. The spatial pattern of the first leading mode shows opposite signs along the southeastern coast and the rest area and the amplitude along the southeastern coast is relatively small for the first epoch, while shows uniform signs over the whole area for the second epoch (not shown). Nevertheless, the first leading mode for the entire period exhibits uniform signs over South China (not shown), thus it is reasonable to compute the reference time series as the temperature averaged over South China.

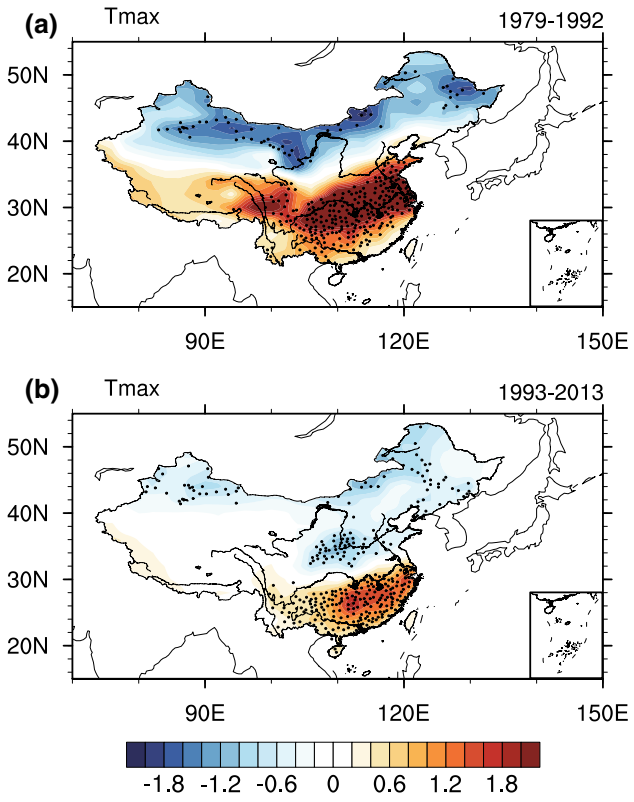

Fig. 4 The same as Fig. 1b, except **a** for the first epoch during 1979–1992 and **b** for the second epoch during 1993–2013

Figure 5 shows the regressed anomalies of 500-hPa geopotential height, wave activity flux and 850-hPa wind against the South China temperature for the two epochs, respectively. For the first epoch from 1979 to 1992, there are significant higher pressure centered over the Korean Peninsula, lower pressure centered to the east of the Lake Baikal and higher pressure around the Ural Mountains (Fig. 5a). The corresponding wave activity flux exhibits southeastward propagation along the three anomaly centers from the Ural Mountains to East Asia, illustrating the influence from the mid-latitude teleconnection. Compared to the whole period as shown in Fig. 2a, the mid-latitude wave train pattern for the first epoch shifts northwards and the East Asian higher pressure is centered north of South China. The higher pressure north of South China is mainly attributable to the mid-latitude influence while the tropical influence is feeble, since the northeastward wave activity flux from the tropics could not reach the higher-pressure center. Consistent with the 500-hPa geopotential height, the regressed 850-hPa wind anomaly shows an anomalous anticyclone around the Korean Peninsula, with the southwestern part stretching to South China (Fig. 5b). Northeasterly anomaly appears over South China, indicating a weaker southwesterly monsoon. Anomalous divergence of water vapor flux occurs over South China but with small significant area (shadings in Fig. 5b), which might favor drier air condition.

For the second epoch from 1993 to 2013, significant higher pressure appears over South China, which is located obviously more southwards compared to the first epoch (Fig. 5c). Meanwhile, there is also a wave train spanning from Europe to East Asia along the mid-latitude, presenting features similar to the whole period but quite different from the first epoch. For the first epoch, the lower pressure near the Lake Baikal is comparable to the higher pressure near the Ural Mountains in terms of magnitude. For the second epoch, the higher pressure around the Ural Mountains elongates more eastwards to Northeast Asia while the lower pressure around the Lake Baikal shrinks and gets much weaker, leading to weaker connection between the mid-latitude and low-latitude regions. Correspondingly, the wave activity flux during the second epoch shows much smaller southeastward propagation from the Ural Mountains to East Asia, suggesting that the influence from the mid-latitude is weaker than the first epoch. However, the East Asian higher pressure for the second epoch remains quite strong and shifts southwards to center over South China. The formation of significant

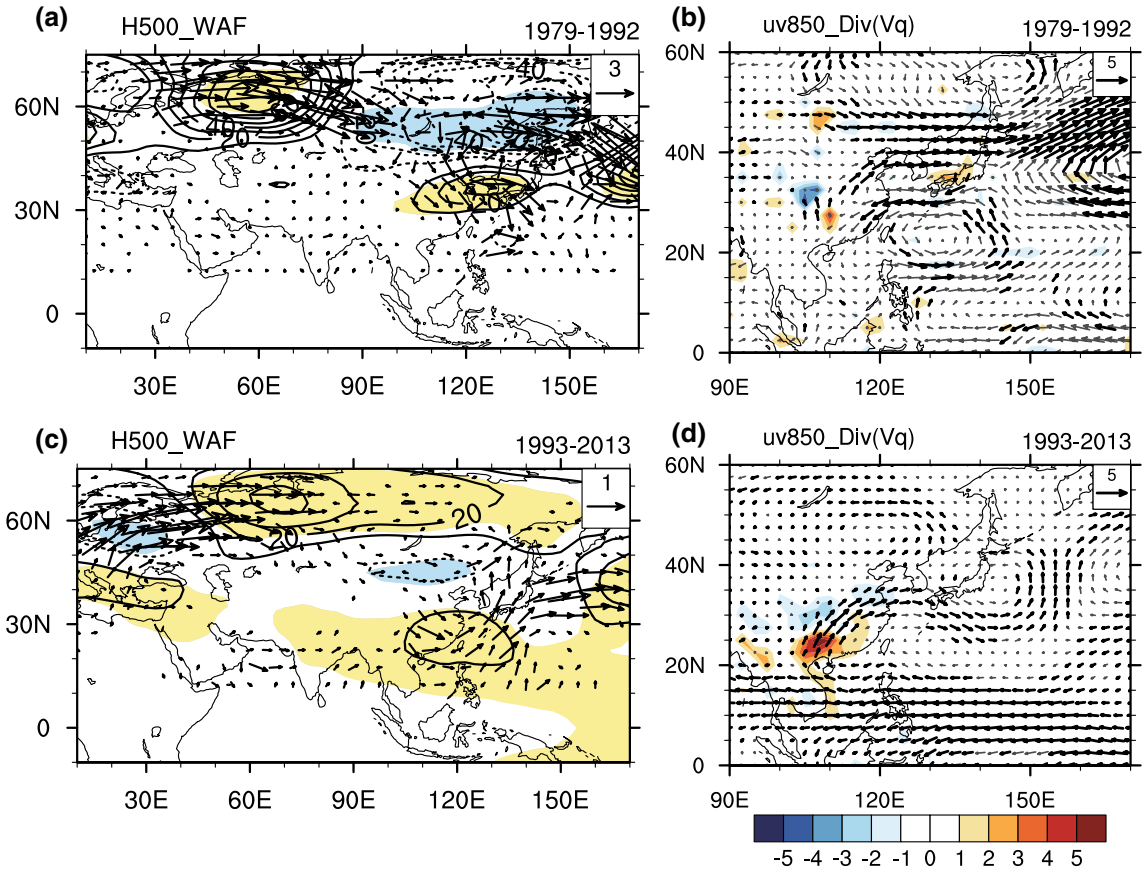

Fig. 5 **a** and **c** are the same as Fig. 2a, except **a** for the first epoch during 1979–1992 and **c** for the second epoch during 1993–2013. **b** and **d** are the regressed anomalies of 850-hPa wind (vectors; units: m s^{-1}; the black vectors are significant) and water vapor flux divergence (shadings; units: 10^{-5} g kg^{-1} s^{-1}; only the significant areas are plotted) against the mid-summer temperature anomaly in South China during 1979–1992 and 1993–2013, respectively

higher pressure over South China is accompanied by the northeastward wave activity flux from the tropics, suggesting that the tropical disturbance plays an important role in the second epoch. In the lower troposphere, the regressed anomaly of 850-hPa wind shows a significant anticyclone over South China, with strong southwesterly anomaly prevailing in the west and north of South China (Fig. 5d). The anomalous southwesterly would enhance the summer monsoon. The enhanced southwesterly increases the northward water vapor transport and results in anomalous divergence of water vapor flux over South China (shadings in Fig. 5d), which could favor anomalous dry air condition and high air temperature.

To specify the main processes contributing to the temperature variations in South China, the regressed anomalies of vertical velocity, specific humidity, total cloud cover, surface net downward shortwave radiation, vertical adiabatic heating and horizontal temperature advection are analyzed (Fig. 6). Associated with the higher pressure, stronger subsidence and lower humidity occur throughout the whole troposphere along the meridional section averaged between 110°E–120°E (Fig. 6a, b). For the first epoch, the subsiding and dry anomalies are centered near 30°N, but also extend southwards to South China located at 20°N–28°N. In contrast, for the second epoch the anomalous centers are located around 25°N and over South China, which are more southward in comparison with the first epoch. The displacements of anomalous centers between the two epochs are in agreement with the different positions of the East Asian higher pressure and higher temperature centers. The anomalous subsidence and dry air condition lead to less cloud cover and more solar radiation at the surface, which is significant for both epochs (Fig. 6c, d). Meanwhile, the anomalous subsidence might bring stronger vertical adiabatic heating. However, the significant enhancement of vertical adiabatic heating occurs over South China only during the second epoch, while occurs over the Yangtze River during the first epoch (contours in Fig. 6e, f). The horizontal temperature advection shows negative anomalies over South China for both epochs (shadings in Fig. 6e, f), which is unfavorable for higher temperature. Therefore, the temperature variation over South China is mainly determined by the shortwave

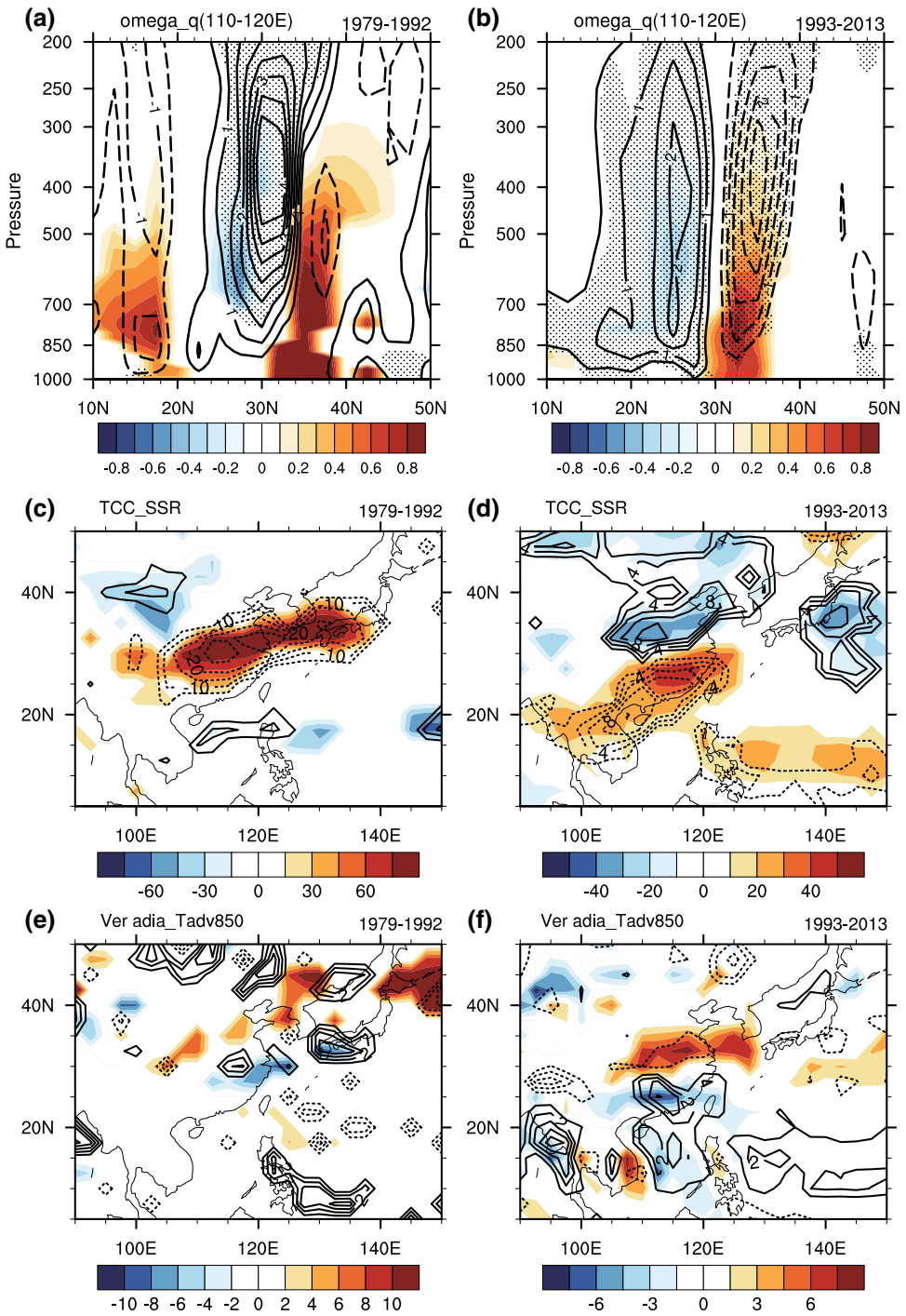

Fig. 6 Regressed anomalies of **a, b** vertical velocity omega (contours; unit: 10^{-4} hPa s^{-1}; the dotted areas are significant) and specific humidity (shading; unit: g kg^{-1}; only the significant areas are shaded) along the meridional section average between 110°E and 120°E, **c, d** Total cloud cover (contours; units: %) and surface net downward shortwave flux (shadings; units: W s^{-1}), **e, f** 850-hPa vertical adiabatic heating (contours; units: 10^{-5} K s^{-1}; contour intervals are 1×10^{-5} K s^{-1}) and 850-hPa horizontal temperature advection (shadings; units: 10^{-6} K s^{-1}). Only the significant areas are plotted in **c**–**f**. The anomalies are regressed against the mid-summer temperature anomaly in South China during the first epoch 1979–1992 (left panels) and the second epoch 1993–2013 (right panels)

radiation before the early 1990s, and by the shortwave radiation and vertical adiabatic heating after the early 1990s.

The simultaneous tropical SSTA and precipitation anomaly associated with the South China temperature variations in the two epochs are compared, and the SSTA in the preceding winter is also analyzed (Fig. 7). For the first epoch, there are only small significant areas scattering over the tropical Pacific (Fig. 7a, c, e). In the mid-summer, negative (positive) SSTA and less (more) precipitation occur over the central (western) tropical Pacific but with low significance level (Fig. 7c, e). In comparison, the regressed anomalies of SST and precipitation for the second epoch appear to be much more significant over the tropical Pacific (Fig. 7b, d, f). The SSTA evolves from an El Niño pattern in the preceding winter to a La Niña pattern in the mid-summer (Fig. 7b, d). Significantly less (more) precipitation occurs over the central–eastern (western) tropical Pacific in the mid-summer (Fig. 7f), which would act as anomalous heat source

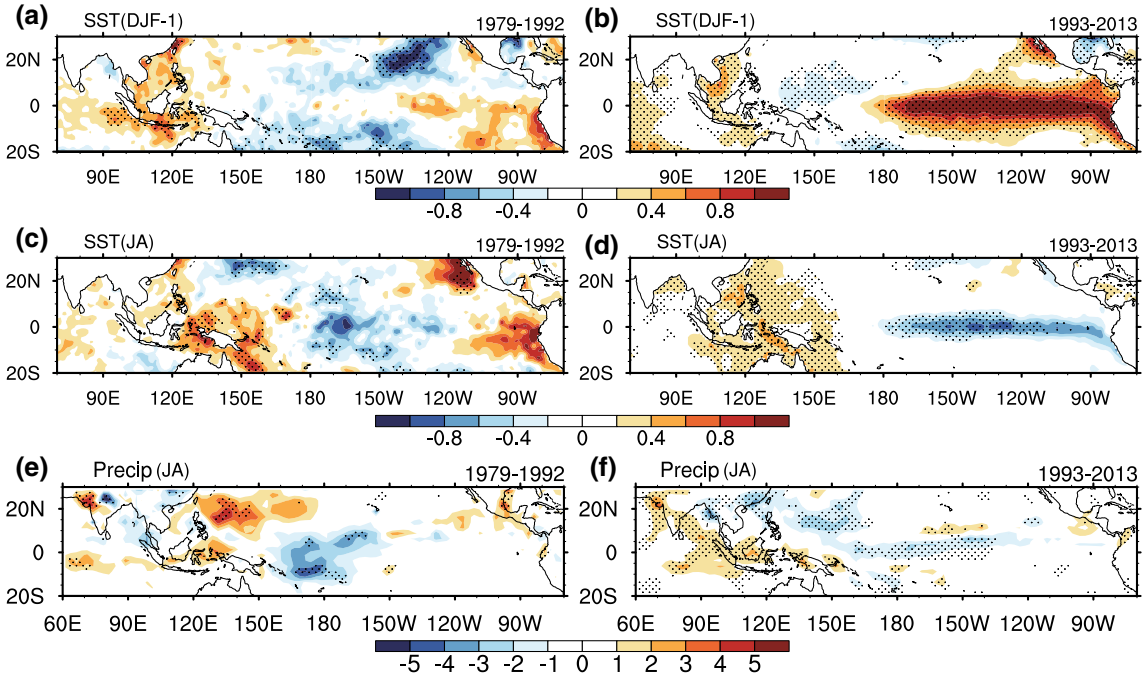

Fig. 7 Regressed anomalies of **a, b** SST in the preceding winter (units: °C), **c, d** SST in the simultaneous mid-summer (units: °C) and **e, f** precipitation in the simultaneous mid-summer (units: mm d^{-1}). The anomalies are regressed against the mid-summer temperature anomaly in South China during the first epoch 1979–1992 (left panels) and the second epoch 1993–2013 (right panels). The dotted areas are statistically significant at the 90% significant level

influencing the atmospheric circulation. It is thus implied that the influence of tropical SSTA on the temperature variation over South China during the second epoch is much more significant than the first epoch. The anomalous patterns for the second epoch are quite similar to the patterns for the whole period from 1979 to 2013 (Fig. 3a, b), indicating that the connection between the tropical Pacific SST and South China temperature is mainly due to their significant correlation after the early 1990s.

The SSTA over the tropical Pacific would modulate the East Asian monsoon circulation and thus influence the South China temperature. The warmer SST over the central–eastern Pacific during the preceding winter could trigger an anomalous lower-tropospheric anticyclone over the western North Pacific and maintain it until early summer (Wang et al. 2000). The further persistence of the anticyclonic anomaly throughout the summer might be favored by the colder summer SST over the central–eastern Pacific during El Niño to La Niña transition years, through a Rossby-wave response (Chen et al. 2015). At the same time, the warmer summer SST over the western tropical Pacific may induce anomalous ascent in situ, which may result in anomalous descent and lower-level anticyclone over the western North Pacific via a local Hadley circulation. For both epochs, an anomalous anticyclone is observed over the western North Pacific (Fig. 5b, d). The anticyclone for the first epoch is located at the low-latitude region east of the Philippines and Indonesia, which may contribute to the anomalous low-level anticyclone over eastern China via a meridional wave-train pattern (Fig. 5b). But the circulation anomalies at the low latitude show low significance level during the first epoch. In contrast, the anticyclone for the second epoch is located to the east of South China, which is obviously more northward and with much higher significance level (Fig. 5d). This difference is related to the more significant SSTA and precipitation anomaly during the second epoch and confirms the stronger influence of tropical SSTA on South China temperature after the early 1990s. The relative contribution of the negative SSTA over the central–eastern tropical Pacific and the positive SSTA over the western tropical Pacific to the anomalous atmospheric circulation over South China would be further investigated based on observational analysis and model simulations. Here we focus on the second epoch when the tropical SSTA plays a more significant role.

Figure 8 displays the regressed anomalies of OLR, surface downward shortwave radiation and downward latent heat flux against the South China temperature for the second epoch. There are significantly negative anomalies of OLR, downward shortwave radiation and downward latent heat flux over the western tropical Pacific, manifesting a stronger convection due to the warmer underlying SST (Fig. 8a–c). In contrast, positive anomalies of OLR, downward shortwave

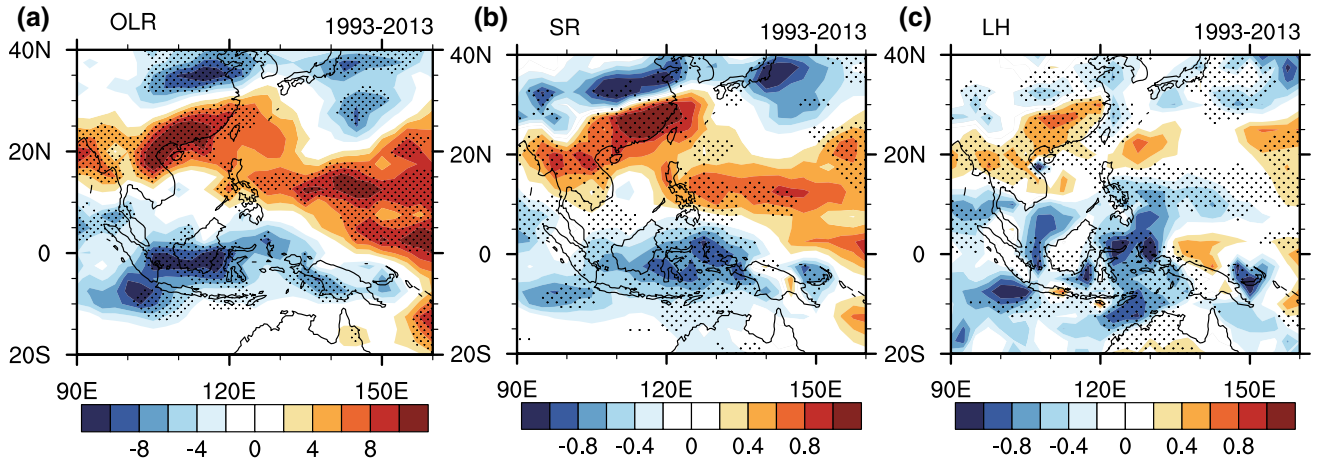

Fig. 8 Regressed anomalies of the **a** outgoing longwave radiation, **b** downward shortwave radiation and **c** downward latent heat flux against the mid-summer temperature anomaly in South China for the second epoch during 1993–2013. Units: W m^{-2}. The dotted areas are significant

radiation and downward latent heat flux occur at the regions north of 10°N, covering the western North Pacific, northern South China Sea and South China. It can be inferred that the SSTA north of 10°N is a response to the atmospheric circulation, since weaker convection would result in less cloud cover, more solar radiation at surface and thus warmer SST. Therefore, for the CAM4 sensitivity simulations which would be presented later, warmer SST over the western Pacific is only imposed within 10°S–10°N, which is also consistent with the key SST region chosen in Fig. 3b.

The stronger convection over the western tropical Pacific triggers an anomalous local Hadley circulation with the descending motion appearing between 20°N–30°N, which is favorable for the higher pressure over South China (Fig. 9a). It is noticeable that the tropical ascending motion is constrained to south of 10°N, confirming that the warmer SST south of 10°N plays an active role to influence the atmospheric circulation. Furthermore, the convection over the western tropical Pacific is also enhanced by the colder SST over the center–eastern Pacific through an anomalous Walker circulation. The regressed anomaly of zonal circulation averaged between 10°S and 10°N shows significant descending over the central Pacific and ascending over the western Pacific (Fig. 9b). Therefore, both the SSTA over the western Pacific and central–eastern Pacific play a role in the anomalous atmospheric circulation associated with South China temperature variation.

In order to compare the relative role of the western Pacific warming and central–eastern Pacific cooling, CAM4 model is employed to perform a control experiment (CTL run) and three sensitivity experiments forced by different SSTA patterns (WP_EP run, WP run and EP run; Fig. 10a–c). Detailed descriptions of the experiments are presented in Sect. 2.2. The difference between the WP_EP run and CTL run would manifest the combining effect of the western Pacific warming and central–eastern Pacific cooling on the circulation anomaly, while the WP run and EP run separately evaluate the effect of western Pacific warming and central–eastern Pacific cooling. The circulation anomaly response to the WP_EP run obtains a significant 850-hPa

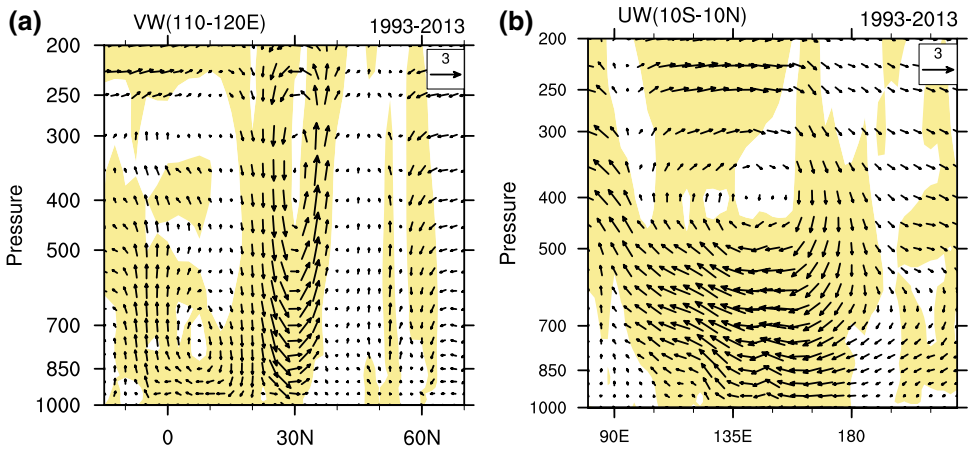

Fig. 9 Regressed anomalies of the **a** meridional vertical circulation averaged between 110°E and 120°E and **b** zonal vertical circulation averaged between 10°S and 10°N against the mid-summer temperature anomaly in South China for the second epoch during 1993–2013. The units are m s^{-1} for the horizontal velocity and -10^{-4} hPa s^{-1} for the vertical velocity omega. The shaded areas are significant either for the horizontal or vertical velocity

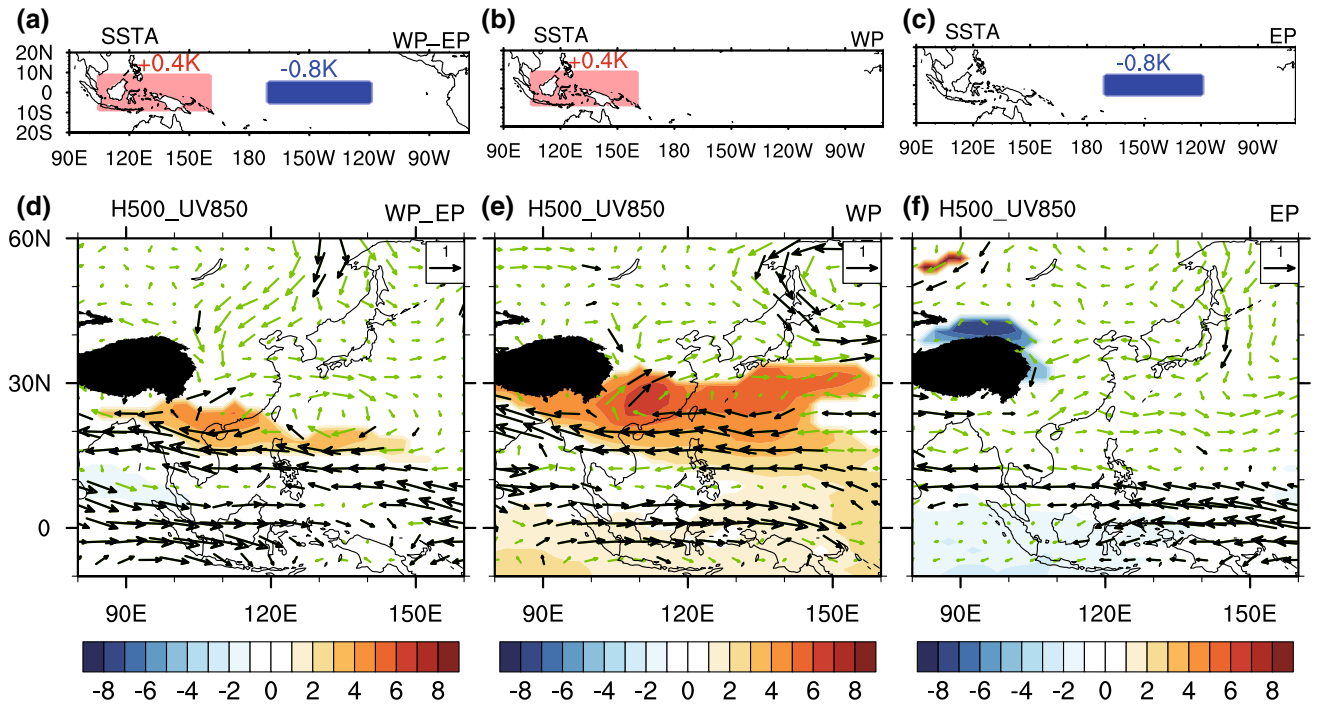

Fig. 10 SSTA imposed to the sensitivity experiments: **a** WP_EP run, **b** WP run and **c** EP run. The anomalous region is (10°S–10°N, 105°E–160°E) over the western Pacific and (5°S–5°N, 170°W–120°W) over the central-eastern Pacific. **d** and **e** are the differences of 500-hPa geopotential height (shading; units: gpm; only the significant areas are shaded) and 850-hPa wind (vectors; units: m s^{-1}; the black vectors are significant) between the sensitivity experiments and the control run

anticyclone and 500-hPa higher pressure over South China (Fig. 10d). This circulation pattern is similar to the observation (Fig. 5c, d), confirming that the concurrence of warmer SST over the western tropical Pacific and colder SST over the central–eastern Pacific favors higher pressure over South China. The WP run also obtains a significant 850-hPa anticyclonic anomaly and 500-hPa higher pressure over South China, which is located more northwards compared to the WP_EP run (Fig. 10e). It is thus indicated that the western Pacific warming is vital for the circulation anomaly over South China. In contrast, the EP run exhibits an 850-hPa anticyclonic anomaly over the western North Pacific with only significant easterly in the southern edge, and the 500-hPa geopotential height anomaly is quite weak (Fig. 10f). The 850-hPa anticyclonic anomaly is similar to the simulating result of Chen et al. (2015), which suggested that the colder summer SST over the central–eastern Pacific is important for maintaining the anticyclonic anomaly over the western North Pacific throughout summer during El Niño to La Niña transition years. However, the anticyclone excited by the central–eastern Pacific cooling is mostly located over the ocean, while the direct effect on the circulation anomaly over South China is weak. On the other hand, the anomalous Walker circulation is only significant for the WP_EP run, while not complete for either the WP run or EP run (not shown). Therefore, it is suggested that the western tropical Pacific SST could remarkably influence the atmospheric circulation over South China via the local Hadley circulation modulated by the convection over the topics, while the central–eastern Pacific SST exerts an indirect impact by influencing the convection over the western tropical Pacific through the Walker circulation.

The above results reveal the important role of the western tropical Pacific SSTA, which is much more significant for the second epoch than for the first epoch. Thus we further examine the SSTA evolutions associated with the western tropical Pacific SSTA for the two epochs, respectively. Figure 11 shows the regressed SSTA during the preceding winter, spring and simultaneous mid-summer against the western tropical Pacific SSTA averaged over the key region (10°S–10°N, 105°E–160°E). For the first epoch, there is negative (positive) SSTA over the central–eastern (western) Pacific, which gradually strengthens from the preceding winter to spring and to summer (Fig. 11a–c). In contrast, for the second epoch, significantly positive (negative) SSTA occurs over the central–eastern (western) Pacific in the previous winter, and then gradually weakens from winter to spring, and transforms into the opposite phase from spring to summer (Fig. 11d–f). It is shown that the warmer mid-summer SST over the western tropical Pacific is related to the La Niña developing phase for the first epoch, while the El Niño to La Niña transition phase for the second epoch. Putting

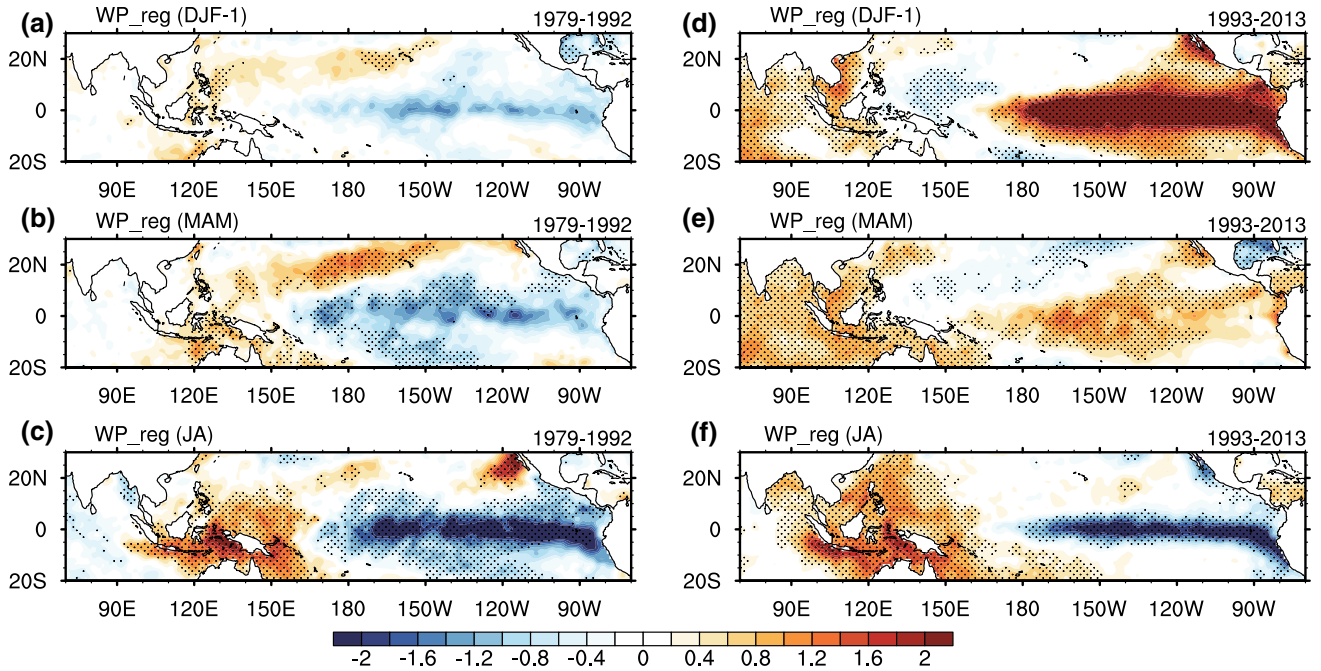

Fig. 11 Regressed SSTA in the preceding winter (December–January), spring (March–May) and simultaneous mid-summer (July–August) against the mid-summer SSTA averaged over the western tropical Pacific key region (10°S–10°N, 105°E–160°E) (units: °C). **a**–c are for the first epoch during 1979–1992 and **d**–**f** are for the second epoch during 1993–2013. The dotted areas are significant

Figs. 11 and 7 together, it is clear that the SSTA pattern related to the western tropical Pacific SSTA for the second epoch are quite similar to the pattern related to the temperature anomaly over South China. Therefore, it is implied that the intimate relationship between the western tropical Pacific SSTA and South China temperature anomaly occurs in the summers during El Niño to La Niña transition years, which is significant since the early 1990s.

5 Conclusions

The current study reveals that the atmospheric circulation and tropical SSTA pattern responsible for the interannual variation of mid-summer temperature in South China experience an obvious interdecadal change around the early 1990s. For the whole period from 1979 to 2013, the temperature anomaly in South China is attributable to the influence from both the extratropical atmospheric circulation and tropical Pacific SSTA. On the one hand, warmer summer in South China is related to a mid-latitude teleconnection with higher-pressure centers over South China and the Ural Mountains and lower-pressure centers south of the Lake Baikal and over Europe. On the other hand, the tropical Pacific SSTA associated with warmer summer in South China is featured by an El Niño pattern in the preceding winter and a La Niña pattern in the simultaneous mid-summer, appearing as the El Niño to La Niña transition phase. However, the above relationship is only significant after 1993, so the atmospheric circulation and tropical Pacific SSTA responsible for the South China temperature variation are compared for the two epochs before and after 1993.

For the first epoch before 1993, the interannual variation of South China temperature is significantly influenced by the extratropical teleconnection while the tropical SSTA presents relatively weak signal. The extratropical teleconnection is located more northwards compared to the whole period, featured by higher pressure around the Ural Mountains, lower pressure east of the Lake Baikal and higher pressure around the Korean Peninsula. Along with the mid-latitude teleconnection, obvious wave activity flux propagates southeastwards from the Ural Mountains to East Asia. South China is located at the southern flank of an anomalous high pressure. The higher pressure results in stronger subsidence and lower humidity throughout the whole troposphere, which decreases the cloud cover and increases the solar radiation at the surface and thus leads to higher air temperature. All the anomalous centers are located to the north of South China with the anomalous scope extending to South China.

For the variation of South China temperature during the second epoch after 1993, the influence of tropical SSTA is much more significant while the influence of mid-latitude atmospheric circulation is weaker compared with the first epoch. The extratropical teleconnection is much weaker during the second epoch, denoted by the smaller magnitude and extension of the lower pressure around the Lake

Baikal. Correspondingly, the southeastward wave activity flux propagating from the mid-latitude region to the low-latitude region is much weaker. However, there is significant higher pressure centered over South China, which is located much more southwards in comparison with the first epoch. The formation of higher-pressure center over South China is favored by the influence from the tropics, manifested by the obvious northeastward wave activity flux from the low-latitude region to South China. The higher pressure results in stronger subsidence and lower humidity centered over South China. On the one hand, the anomalous subsiding and dry air condition reduce the cloud cover and enhance solar radiation at the surface and thus favor higher air temperature, which is similar to the first epoch. On the other hand, the anomalous subsidence brings stronger vertical adiabatic heating over South China and thus further increases the air temperature, which is insignificant in the first epoch.

The SSTA associated with the variation of South China temperature during the first epoch shows small significant areas scattering over the tropical Pacific, suggesting a relatively weak influence on the circulation over South China. In contrast, the tropical Pacific SSTA associated with higher South China temperature during the second epoch significantly presents the El Niño to La Niña transition phase, which is similar to the whole period. The relative contribution of the western Pacific warming and central–eastern Pacific cooling during the mid-summer in the second epoch to the formation of higher pressure over South China is further investigated, based on the observational analysis and model simulations with CAM4. The results show that the warmer SST over the tropical western Pacific would trigger a local Hadley circulation with stronger convection over the tropics and subsidence over South China, the latter of which would directly lead to higher pressure over South China. As for the colder SST over the central–eastern Pacific, the Rossby-wave response to the cooling presents weak signal over South China. Instead, the central–eastern Pacific cooling would favor an anomalous Walker circulation and enhance the convection over the western tropical Pacific. It is thus indicated that the central–eastern Pacific plays an indirect role in influencing the South China temperature.

The influence of the western tropical Pacific SSTA on the South China temperature for the second epoch is much more significant than that for the first epoch, and it is related to the difference in the accompanying SSTA pattern over the tropical Pacific. The warmer SST in summer over the western tropical Pacific is associated with the El Niño to La Niña transition phase for the second epoch while La Niña developing phase for the first epoch. On the other hand, the El Niño to La Niña transition phase is favorable for the occurrence of warmer summer in South China. Thereby, the relationship between the tropical Pacific SSTA and South China temperature is built for the second epoch. It is implied that the mid-summer temperature of South China is more predictable during the El Niño to La Niña transition years, which is the case for the recent decades since the early 1990s.

Acknowledgements This work is jointly supported by National Key R&D Program of China (2016YFA0600601), National Natural Science Foundation of China (Grant Nos. 41605027, 41530530 and 41320104007).

References

Chen Z, Wen Z, Wu R et al (2015) Relative importance of tropical SST anomalies in maintaining the Western North Pacific anomalous anticyclone during El Niño to La Niña transition years. Clim Dyn 46:1027–1041

Chen R, Wen Z, Lu R (2016) Evolutions of the circulation anomalies and the quasi-biweekly oscillations associated with extreme heat events in South China. J Clim 29:6909–6921

Chen J, Wen Z, Wu R et al (2017) An interdecadal change in the intensity of interannual variability in summer rainfall over southern China around early 1990s. Clim Dyn 48:191–207

Dee D, Uppala S, Simmons A et al (2011) The ERA-interim reanalysis: configuration and performance of the data assimilation system. Q J R Meteorol Soc 137:553–597

Ding T, Qian W (2012) Statistical characteristics of heat wave precursors in China and model prediction. Chin J Geophys 55:1472–1486 **(Chinese)**

Ding Y, Wang Z, Sun Y (2008) Inter-decadal variation of the summer precipitation in East China and its association with decreasing Asian summer monsoon. Part I: observed evidences. Int J Climatol 28:1139–1161

Gao R, Wang L, Gao G (2008) The trend of variation in high temperature days during 1956–2006 in China. Adv Clim Change Res 4:177–181 **(Chinese)**

Gong D, Pan Y, Wang J (2004) Changes in extreme daily mean temperatures in summer in eastern China during 1955–2000. Theor Appl Climatol 77:25–37

He F, Xu J, Zhou W et al (2008) Evaluation on effects of meteorological conditions on electrical comsumption in megathermal days of Shanghai. Plateau Meteorol 27(Suppl):210–217 **(Chinese)**

Hu Z (1997) Interdecadal variability of summer climate over East Asia and its association with 500 hPa height and global sea surface temperature. J Geophy Res Atmos 102(D16):19403–19412

Kwon M, Jhun J, Wang B et al (2005) Decadal change in relationship between east Asian and WNP summer monsoons. Geophys Res Lett 32:101–120

Kwon M, Jhun J, Ha K (2007) Decadal change in east Asian summer monsoon circulation in the mid-1990s. Geophys Res Lett 34:377–390

Li T, Du Y, Mo Y et al (2014) Human health risk assessment of heat wave based on vulnerability: a review of recent studies. J Environ Health 31:547–550 **(Chinese)**

Li Z, Cao L, Zhu Y, Yan Z (2016) Comparing two homogenized datasets of daily maximum/mean/minimum temperatures in China during 1960–2013. J Meteorol Res 30:53–66

Liebmann B, Smith C (1996) Description of a complete (interpolated) outgoing longwave radiation dataset. Bull Am Meteorol Soc 77:1275–1277

Luo Q, Ji Z (2005) Climatological analysis of anomalous summer temperature patterns in Guangdong province. J Trop Meteorol 21:427–434 **(Chinese)**

Neale R, Richter J, Park S et al (2013) The mean climate of the community atmosphere model (CAM4) in forced SST and fully coupled experiments. J Clim 26:5150–5168

Rayner N, Parker D, Horton E et al (2003) Global analyses of sea surface temperature, sea ice, and night marine air temperature since the late nineteenth century. J Geophys Res 108:1063–1082

Ren G, Shen A, Ling C (2011) Cause and forecast of abnormal temperature in southern China during midsummer. J Meteorol Res Appl 32:1–5 **(Chinese)**

Sui C, Chung P, Li T (2007) Interannual and interdecadal variability of the summertime western North Pacific subtropical high. Geophys Res Lett 34:93–104

Sun J, Wang H, Yuan W (2011) Decadal variability of the extreme hot event in China and its association with atmospheric circulations. Clim Environ Res 16:199–208 **(in Chinese)**

Wang B, Wu R, Fu X (2000) Pacific–East Asian teleconnection: how does ENSO affect East Asian climate? J Clim 13:1517–1536

Wang B, Huang F, Wu Z et al (2009) Multi-scale climate variability of the South China sea monsoon: a review. Dyn Atmos Oceans 47:15–37

Wang W, Zhou W, Wang X et al (2013) Summer high temperature extremes in Southeast China associated with the East Asian jet stream and circumglobal teleconnection. J Geophy Res Atmos 118:8306–8319

Wang W, Zhou W, Li X et al (2016) Synoptic-scale characteristics and atmospheric controls of summer heat waves in China. Clim Dyn 46:2923–2941

Wei K, Chen W (2009) Climatology and trend of high temperature extremes across China in summer. Atmos Ocean Sci Lett 2:153–158

Wu R, Wen Z, Yang S, Li Y (2010) An interdecadal change in southern China summer rainfall around 1992/93. J Clim 23:2389–2403

Yan L, Huang X (2005) On anomalous climatic change of South China temperature in July. Meteorology 31:64–67 **(in Chinese)**

Yang H, Li C (2005) Diagnostic study of serious high temperature over South China in 2003 summer. Clim Environ Res 10:80–85 **(in Chinese)**

Yim S, Jhun J, Yeh S (2008) Decadal change in the relationship between east Asian-western North Pacific summer monsoons and ENSO in the mid-1990s. Geophys Res Lett 35:229–237

Yim S, Wang B, Kwon M (2014) Interdecadal change of the controlling mechanisms for East Asian early summer rainfall variation around the mid-1990s. Clim Dyn 42:1325–1333

Zeng J, Zhai Y, Wu Z, Hu K (2011) Effects of high temperature in summer on yield and its components in bitter gourd with 15 cross combinations and strains. Chin J Trop Crops 32:2025–2028 **(in Chinese)**

Zhang H, Wen Z, Wu R et al (2016) Inter-decadal changes in the East Asian summer monsoon and associations with sea surface temperature anomaly in the South Indian Ocean. Clim Dyn. https://doi.org/10.1007/s00382-016-3131-6